JACS
JOURNAL OF THE AMERICAN CHEMICAL SOCIETY

ARTICLE

pubs.acs.org/JACS

End-to-End Coupling and Network Formation Behavior of Cylindrical Block Copolymer Micelles with a Crystalline Polyferrocenylsilane Core

Siti F. Mohd Yusoff,[†,‡] Joe B. Gilroy,[†] Graeme Cambridge,[§] Mitchell A. Winnik,[*,§] and Ian Manners[*,†]

[†]School of Chemistry, University of Bristol, Bristol, United Kingdom BS8 1TS

[‡]Universiti Kebangsaan Malaysia, 43600 UKM Bangi, Selangor, Malaysia

[§]Department of Chemistry, University of Toronto, 80 St. George Street, Toronto, Ontario, Canada M5S 3H6

Supporting Information

ABSTRACT: Cylindrical block copolymer micelles with a crystalline poly(ferrocenyldimethylsilane) (PFDMS) core and a long corona-forming block are known to elongate through an epitaxial growth mechanism on addition of further PFDMS block copolymer unimers. We now report that addition of the semicrystalline homopolymer $PFDMS_{28}$ to monodisperse short (ca. 200 nm), cylindrical seed micelles of PFDMS block copolymers results in the formation of aggregated structures by end-to-end coupling to form micelle networks. The resulting aggregates were characterized by dynamic light scattering (DLS), transmission electron microscopy (TEM), and atomic force microscopy (AFM). In some cases, a core-thickening effect was also observed where the added homopolymer appeared to deposit and crystallize at the core−corona interface, which resulted in an increase of the width of the micelles within the networks. No evidence for aggregation was detected when the amorphous homopolymer poly(ferrocenylethylmethylsilane) ($PFEMS_{25}$) was added to the cylindrical seed micelles whereas similar behavior to $PFDMS_{28}$ was noted for semicrystalline polyferrocenyldimethylgermane ($PFDMG_{30}$). This suggested that the crystallinity of the added homopolymer is critical for subsequent end-to-end coupling and network formation to occur. We also explored the tendency of the cylindrical seed micelles to form aggregates by the addition of PI-*b*-PFDMS (PI = polyisoprene) block copolymers (block ratios 6:1, 3.8:1, 2:1, or 1:1), and striking differences were noted. The results ranged from typical micelle elongation, as reported in previous work, at high corona to core-forming block ratios (PI-*b*-PFDMS; 6:1) to predominantly end-to-end coupling at lower ratios (PI-*b*-PFDMS; 2:1, 1:1) to form long, essentially linear structures. The latter process, especially for the 2:1 block copolymer, led to much more controlled aggregate formation compared with that observed on addition of homopolymers.

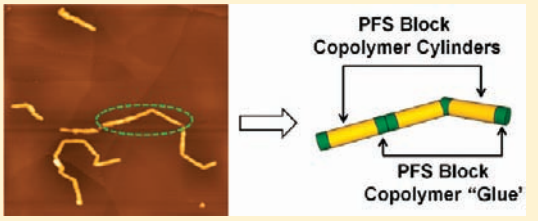

INTRODUCTION

The self-assembly of block copolymers, either in bulk, thin films, or solution, provides an important route to functional nanomaterials with the potential for a variety of applications.[1] Self-assembly of block copolymers in bulk or in thin films is based on the microphase separation of the immiscible blocks which allows access to well-ordered periodic arrays of nanostructures.[2] These nanostructured materials have been utilized to create porous membranes,[3] lithographic templates,[2d,4] and photonic band gap materials.[5] Like traditional surfactants, block copolymers are generally amphiphilic. When block copolymers are dissolved in a block-selective solvent, self-assembly into micelles occurs.[6] Block copolymer micelles have been used as nanoreactors,[7] drug-delivery vehicles,[8] and templates for the fabrication of one-dimensional nanostructures.[1e,9]

High molecular weight polyferrocenylsilanes (PFSs) are an interesting class of transition-metal-containing polymers that are readily available via the ring-opening polymerization (ROP) of monomeric silicon-bridged [1]ferrocenophanes, for example, dimethylsila[1]ferrocenophane **1** (E = Si, R, R′ = Me).[10] Block copolymers containing polyferrocene segments offer interesting possibilities for the preparation of self-assembled architectures with novel properties in the solid state[11] and in solution[12] and have shown utility as lithographic etch resists,[2d,g,13] as redox-active materials,[14] and as precursors to catalytically active or magnetic metal nanoparticles.[11c,15] PFS block copolymers have been well-characterized in bulk and thin films in terms of their morphology.[16] These studies have involved a variety of materials such as polystyrene-*b*-polyferrocenylsilane (PS-*b*-PFS),[2f,16a,16e,16f,17] polyferrocenylsilane-*b*-poly(dimethylsiloxane) (PFS-*b*-PDMS),[16d,g] polyferrocenylsilane-*b*-poly-2-vinylpyridine (PFS-*b*-P2VP),[16c] and polyisoprene-*b*-polyferrocenylsilane (PI-*b*-PFS).[16b]

Solution self-assembly of PFS block copolymers yields well-defined micellar aggregates such as spheres,[16c,18] cylinders,[19] and platelets[20] depending on the relative length of the corona and the core-forming blocks. Asymmetric block copolymers with a crystalline[21] PFS core-forming block generally form cylindrical micelles over a wide range of compositions in which PFS is the shortest block. The tendency to form cylinders has been attributed to a counterbalance of the competing effects of the semicrystalline PFS core and intercoronal chain repulsions,[22] which

Received: March 15, 2011
Published: May 26, 2011

Scheme 1. Elongation of Cylindrical PFDMS Block Copolymer Micelles on Addition of Further (i) PFDMS Block Copolymer with the Same Corona-Forming Block (Top), (ii) PFDMS Block Copolymer with a Different Corona-Forming Block (Center), and (iii) PFDMG Block Copolymer (Bottom)[a]

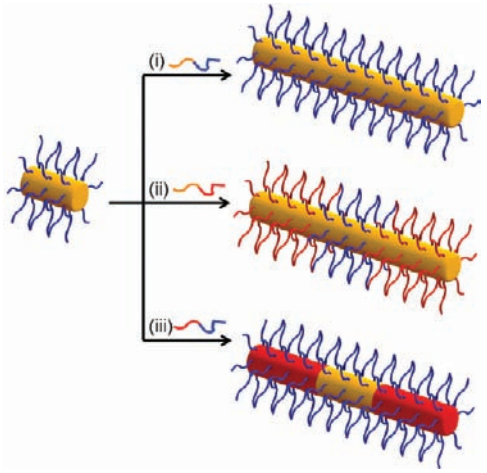

[a] PFDMS is amber, PFDMG is red, and the corona-forming blocks are blue or red.

Scheme 2. Synthesis of PFDMS, PFEMS, and PFDMG Homopolymers

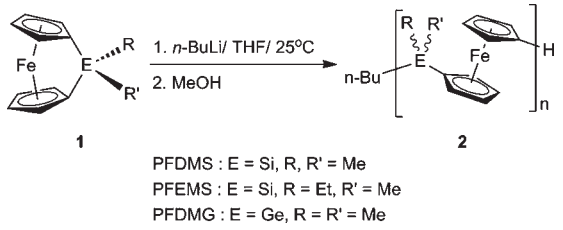

tend to either disfavor or favor core−corona interfacial curvature, respectively.[22−24] Recently, we have discovered a fascinating feature of cylindrical PFS block copolymer micelles with a crystalline PFS core and a long corona-forming block whereby, on addition of further block copolymer, they increase in length by a nucleated homoepitaxial growth mechanism that exhibits many of the characteristics of a living polymerization (Scheme 1, top).[12] Addition of a PFS block copolymer with a different corona-forming block yields B-A-B block comicelles, micelle analogs of block copolymers, where the coronal chemistry is spatially structured with a different composition at the ends of the cylinder compared to the center (Scheme 1, center).[12a,25] Furthermore, the addition of analogous block copolymers with a core-forming polyferrocenylgermane (PFG) block leads to similar elongation via a heteroepitaxial growth process which involves the creation of PFG−PFS heterojunctions in the crystalline micelle core (Scheme 1, bottom).[12b]

To provide further insight into these phenomena, we now report studies of the addition of PFS and PFG homopolymers and also PFS block copolymers with a wide range of block ratios to pre-existing (ca. 200 or 500 nm), narrow length dispersity, cylindrical seed micelles. This work provides an important link

Table 1. Characterization Data for PFDMS, PFEMS, and PFDMG Homopolymers

polymer	theoretical M_n (g/mol)	experimental M_n (g/mol)[a]	PDI[a]	DP_n
$PFDMS_{28}$	5000	6800	1.04	28
$PFDMS_{65}$	14 000	15 700	1.04	65
$PFDMS_{141}$	30 000	34 200	1.03	141
$PFEMS_{25}$	5000	6400	1.03	25
$PFDMG_{30}$	11 400	8400	1.04	30

[a] Determined by multidetection GPC analysis. Subscripts represent number-average degree of polymerization.

Scheme 3. Synthesis of PI-*b*-PFDMS Block Copolymers

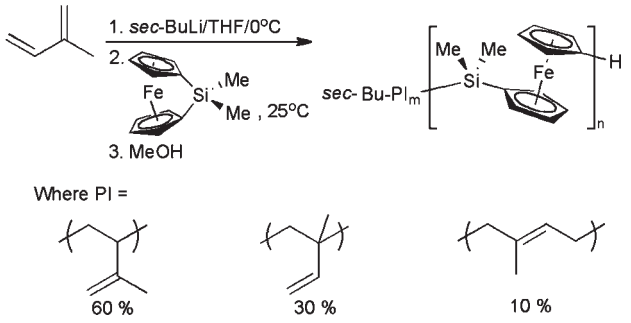

Scheme 4. Synthesis of PFDMS-*b*-PDMS Block Copolymers

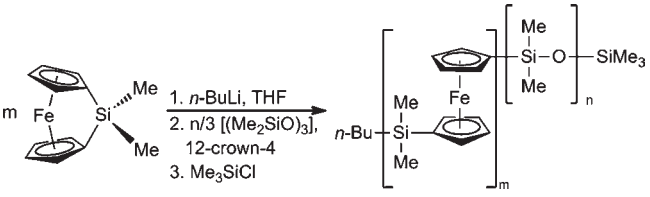

with our previous studies that involved cylinder elongation via the addition of asymmetric PFS block copolymers with a long corona-forming coblock.

RESULTS AND DISCUSSION

1. Synthesis and Characterization of PFS and PFG Homopolymers and PFS Block Copolymers. The poly(ferrocenyldimethylsilane) (PFDMS), poly(ferrocenylethylmethylsilane) (PFEMS), and poly(ferrocenyldimethylgermane) (PFDMG) homopolymers employed in these studies were synthesized via living anionic ROP of the respective [1]ferrocenophane monomers as outlined in Scheme 2.[26] The characterization data for the homopolymers is reported in Table 1 (also see Figure S1 in the Supporting Information). The PI-*b*-PFDMS diblock copolymers were prepared by the addition of dimethylsila[1]ferrocenophane monomer **1** to a solution of living PI synthesized by anionic polymerization of the isoprene monomer with *sec*-BuLi as initiator[19a] and by termination with a few drops of degassed methanol (Scheme 3). A similar sequential living anionic polymerization approach was applied for the synthesis of PFDMS-*b*-PDMS diblock copolymers. This involved the addition of hexamethylcyclotrisiloxane $(Me_2SiO)_3$ containing 12-crown-4 in tetrahydrofuran (THF) to a solution of living PFS prepared from

dimethylsila[1]ferrocenophane initiated with *n*-BuLi (Scheme 4).[26a] The living PFDMS-*b*-PDMS was quenched with a few drops of Me_3SiCl. For both diblock copolymers, an aliquot of the living first blocks (PI and PFDMS) was removed and quenched with degassed methanol in order to obtain a measurement of molecular weight by gel permeation chromatography (GPC). PFDMS diblock copolymers were precipitated into rapidly stirring methanol, and polydispersities (PDIs) of polymers were determined using GPC (see Figure S2 of the Supporting Information). The block ratios and molecular weights of the block copolymers were obtained from ^{1}H NMR spectra (see Figures S3 and S4 of the Supporting Information) via integration of unique signals associated with each of the blocks and comparison to the absolute molecular weight of the homopolymers determined by GPC. The characterization data for the polymers studied here are reported in Tables 1 and 2.

Table 2. Characterization Data for PFDMS Block Copolymers

	first block	block copolymers		
polymer	M_n (g/mol)[a]	M_n (g/mol)[b]	PDI[a]	molar block ratio[b]
PI_{324}-*b*-$PFDMS_{54}$	22 100	36 700	1.07	6:1
PI_{76}-*b*-$PFDMS_{76}$	5100	23 600	1.01	1:1
PI_{200}-*b*-$PFDMS_{100}$	13 600	37 800	1.07	2:1
PI_{296}-*b*-$PFDMS_{77}$	20 100	38 800	1.06	3.8:1
$PFDMS_{37}$-*b*-$PDMS_{258}$	8960	28 100	1.05	1:7

[a] Determined by multidetection GPC analysis. [b] Calculated from relative ^{1}H NMR integration of unique signals for each block. Subscripts represent number-average degree of polymerization.

2. SELF-ASSEMBLY STUDIES

2.1. Homoepitaxial Growth of $PFDMS_{28}$ Homopolymer from Short Cylindrical Seed Micelles with a PFDMS Core. Before homoepitaxial growth studies were conducted, short cylindrical seed micelles of PI_{324}-*b*-$PFDMS_{54}$ block copolymer were prepared in *n*-hexane, which is a selective solvent for the PI block. First, 50 mL of *n*-hexane was added to a vial containing 50 mg of PI_{324}-*b*-$PFDMS_{54}$, which was then sealed and immersed in an oil bath and was heated to 70 °C for 1 h. Next, the resulting clear yellow solution was cooled to room temperature and was allowed to age overnight (16 h). The resulting micelles were studied after solvent evaporation by transmission electron microscopy (TEM) and atomic force microscopy (AFM). A TEM micrograph of the resulting long cylindrical micelles of PI_{324}-*b*-$PFDMS_{54}$ is shown in Figure 1a. We obtained short cylindrical seed micelles of PI_{324}-*b*-$PFDMS_{54}$ with a narrow length distribution and a number average length of L_n = 200 nm (L_w/L_n = 1.05,

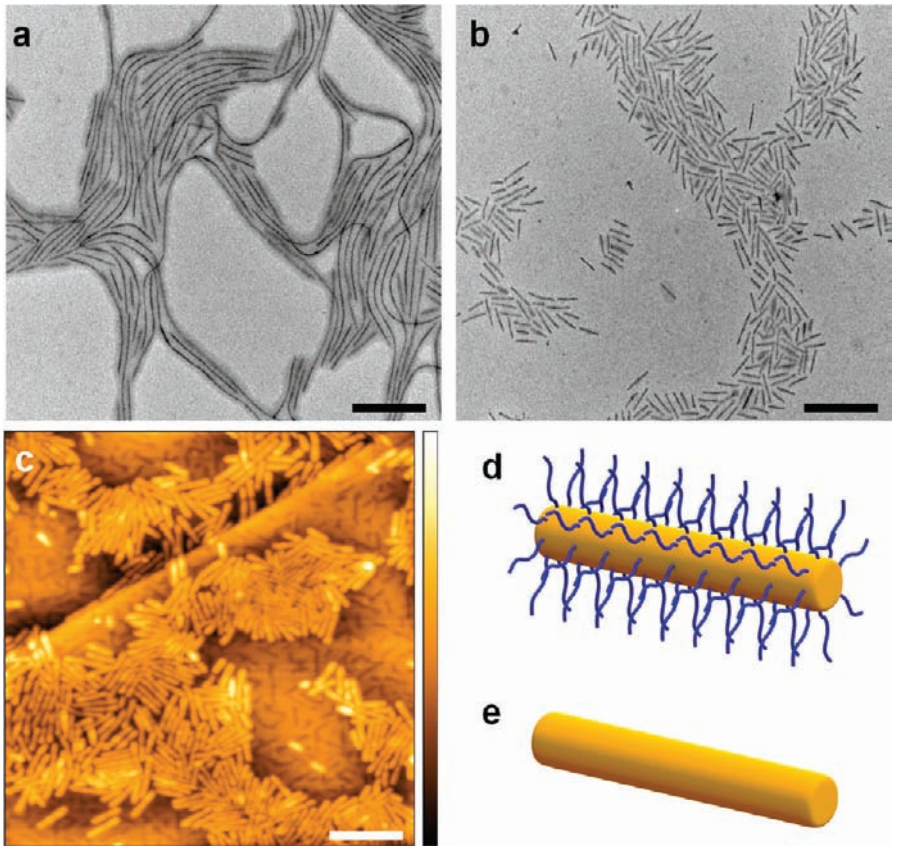

Figure 1. TEM images of (a) cylindrical micelles of PI_{324}-*b*-$PFDMS_{54}$ (the shadow around the dark cores of the cylinders is the PI corona), (b) short (ca. 200 nm), cylindrical seed micelles after sonication, (c) tapping mode AFM height image of short (ca. 200 nm), cylindrical seed micelles drop cast onto freshly cleaved highly ordered pyrolytic graphite (HOPG) (the step observed in the image that runs from left to right at angle of ca. 60° is a feature of the HOPG substrate), (d) schematic representation of seed micelles consisting of an amber PFS core and a blue PI corona, and (e) simplified schematic representation of PFS micelle core for use in subsequent figures. Horizontal scale bars correspond to 500 nm. The vertical scale bar in c corresponds to 0−31 nm.

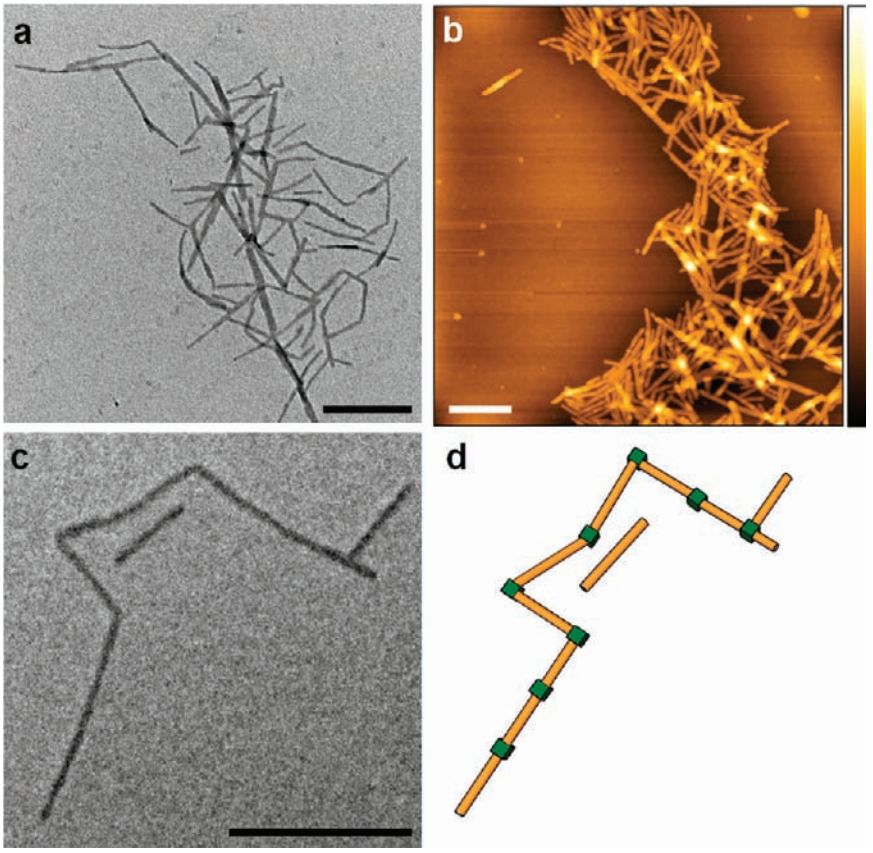

Figure 2. (a) TEM image of micelle networks, (b) tapping mode AFM height image of a solution drop cast onto freshly cleaved HOPG after addition of 15 μg of $PFDMS_{28}$ homopolymer added as 1 mg/mL solution in THF (rms background 0.37 nm), (c) high-magnification TEM image showing the homopolymer acting as a glue for the short, cylindrical seed micelles, and (d) simplified schematic representation of the micelle network observed in TEM image c after addition of $PFDMS_{28}$ homopolymer to PI_{324}-*b*-$PFDMS_{54}$ seed micelles (orange cylinder, PFDMS core of block copolymer micelles; green cubes, added of $PFDMS_{28}$ homopolymer). Horizontal scale bars correspond to 500 nm. The vertical scale bar in b corresponds to 0−50 nm.

$\sigma/L_n = 0.19$) by sonication of a 1 mg/mL *n*-hexane solution of the long PI_{324}-*b*-$PFDMS_{54}$ cylinders at −78 °C for 30 min using a 50W ultrasonic processor equipped with a titanium sonotrode. Representative TEM and AFM images after solvent evaporation are shown in Figure 1b and c, respectively.

To study the effect of the addition of PFS homopolymer to the 200 nm cylindrical PI_{324}-*b*-$PFDMS_{54}$ seed micelles, a stirred solution containing 50 μg of the seed micelles in 1 mL of *n*-hexane was treated with 15 μg of $PFDMS_{28}$ homopolymer delivered as a 1 mg/mL solution in THF, a good solvent for both PFDMS and PI. After 10 s, the stirring was halted and the sample was aged for 1 day. The micelle solution was studied using dynamic light scattering (DLS) and subsequently by TEM and AFM after solvent evaporation. The DLS data indicated a substantial increase in the apparent hydrodynamic radius ($R_{H,app}$) from ca. 70 nm to ca. 500 nm after homopolymer addition, which is consistent with the formation of larger structures (see Figure S5 of the Supporting Information).[27] TEM and AFM images (Figure 2a−c) revealed striking differences from the images obtained for the original short, cylindrical seed micelles (Figure 1b, c) and showed clear evidence of micelle aggregation.

The value for the cross-section of the aggregates from TEM and AFM analysis (several micrometers) was much higher than that with the $R_{H,app}$ value obtained from DLS studies.[28] This suggests that, although significant aggregation occurs in solution, the degree of aggregation may be substantially increased upon solvent evaporation. This assertion is supported by the observation that the aggregates isolated after solvent evaporation could not be redispersed into *n*-hexane to form a stable colloidal solution.

On the basis of the TEM and AFM images, the addition of $PFDMS_{28}$ homopolymer appears to occur primarily at the ends of the short, cylindrical seed micelles. This leads to linkages between often two but also frequently three or more micelles to form networks (Figure 2c and d). Furthermore, close inspection of Figure 2a and b provided evidence that the homopolymer can also competitively add to the core along the long axis of the cylindrical seed micelles leading to core-thickening effects. We will return to this issue later where we will discuss further evidence for this phenomenon.

To study the effect of the addition of different quantities of $PFDMS_{28}$ to the 200 nm cylindrical seed micelles of PI_{324}-*b*-$PFDMS_{54}$, we added a series of increasing amounts of $PFDMS_{28}$ homopolymer as 1 mg/mL solutions in THF to a 1 mL *n*-hexane solution containing 50 μg of short, cylindrical seed micelles. The resulting aggregation was again studied by DLS followed by both TEM and AFM analysis. The DLS studies showed an increase in $R_{H,app}$ with an increase in the quantity of $PFDMS_{28}$ homopolymer added (5 μg and 10 μg of $PFDMS_{28}$ homopolymer), which was consistent with increased aggregation of micelle seeds in solution (see Figure S7 of the Supporting Information). However, upon the further addition of 30 μg

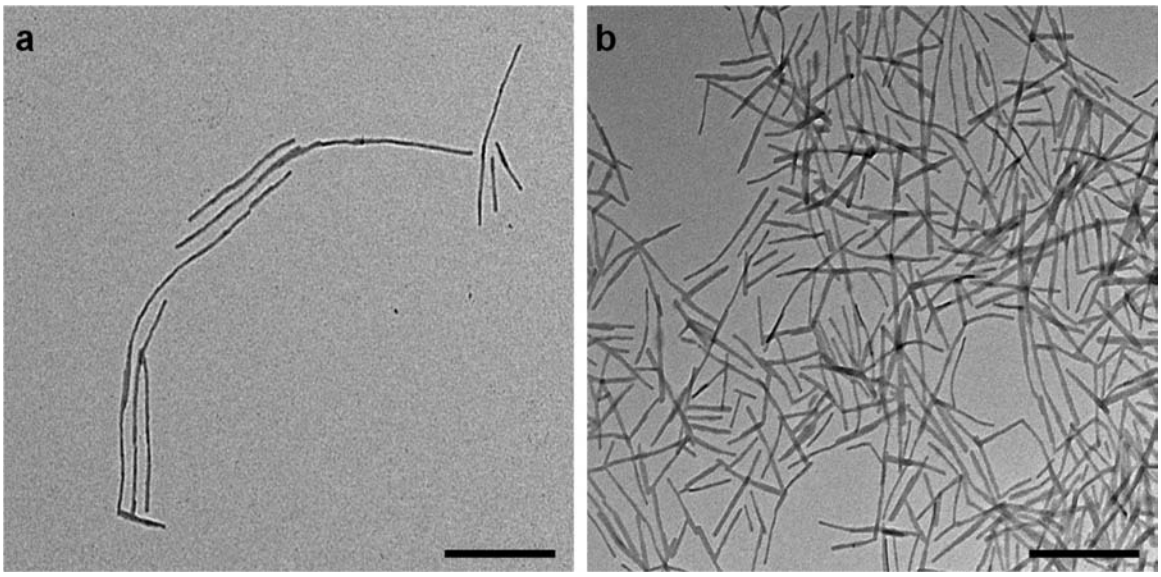

Figure 3. TEM images of aggregated structures formed when (a) 5 μg and (b) 10 μg of $PFDMS_{28}$ homopolymer (added as 1 mg/mL solution in THF) were added to an *n*-hexane solution of short, cylindrical seed micelles of PI_{324}-*b*-PFS_{54}. Scale bars correspond to 500 nm.

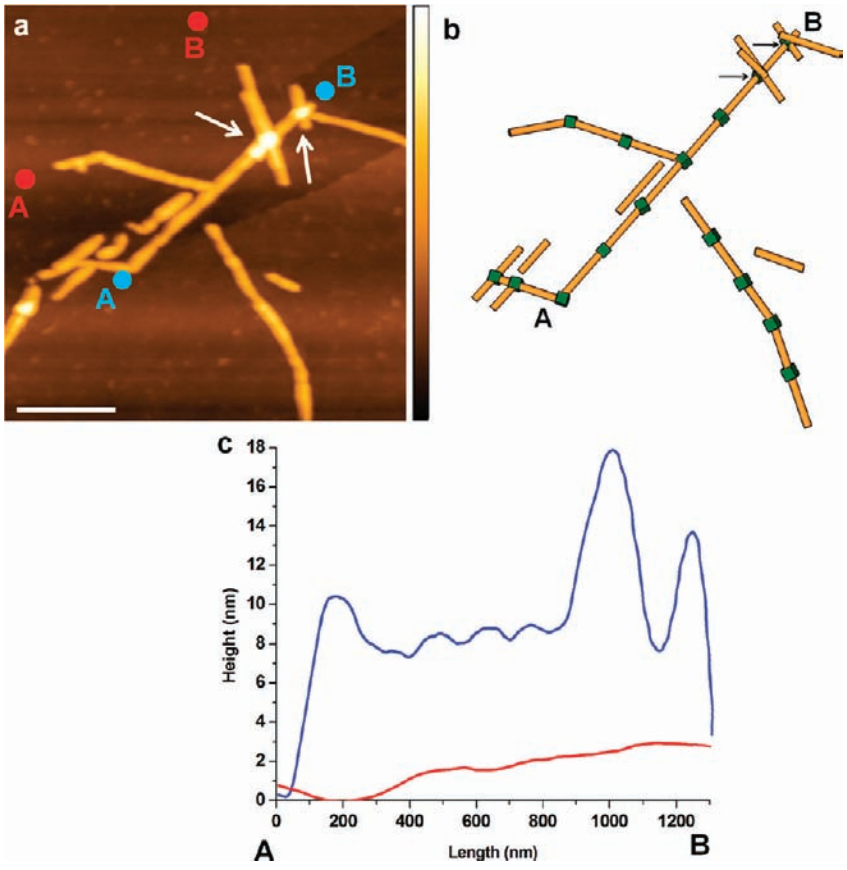

Figure 4. (a) Tapping mode AFM height image, (b) schematic representation of coupled micelles from point A to point B (arrow corresponds to overlapped cylinders), (c) height profile of coupled micelles (blue) and surface background (red) from point A to point B. The sample was prepared by drop casting a micelle solution (concentration 0.05 mg/mL) onto freshly cleaved HOPG (rms background 0.61 nm). The length of the coupled micelle (blue) is approximately 1200 nm, which is consistent with six short, cylindrical seed micelles connecting in a linear fashion. Near point B, we observe an increase in height which represents overlapping cylinders (white arrows). Horizontal scale bar corresponds to 500 nm. Vertical scale bar in a corresponds to 0−21 nm.

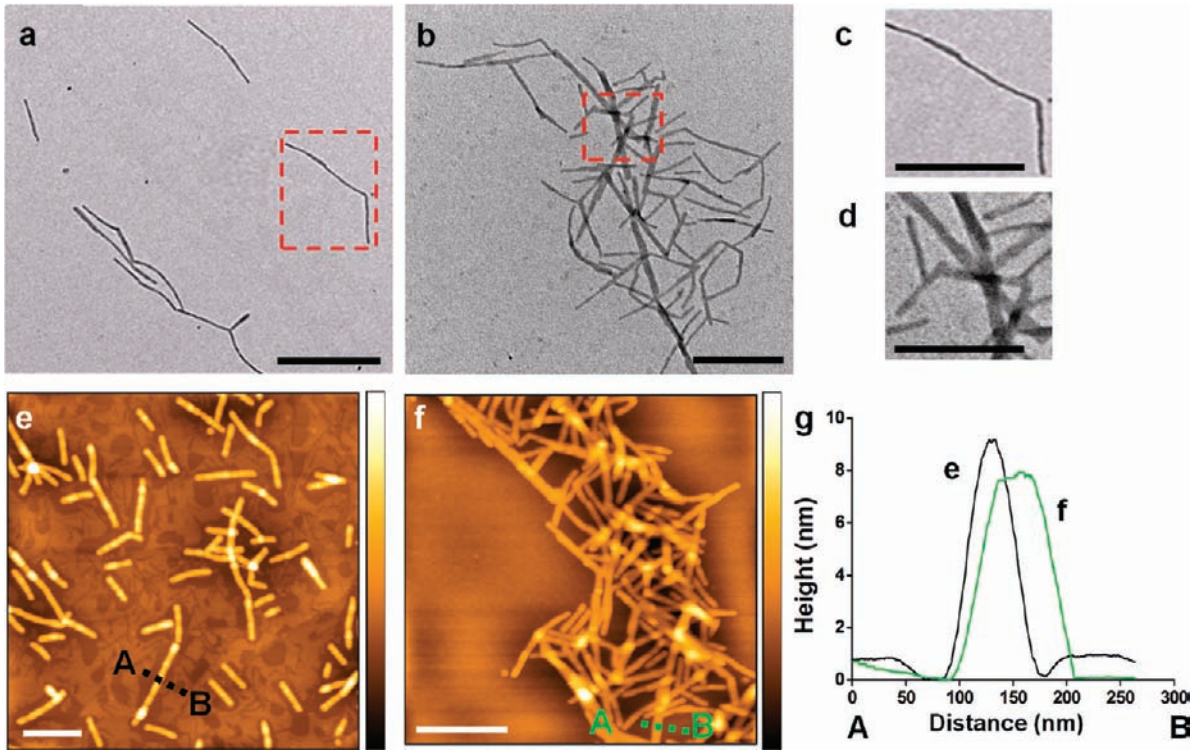

Figure 5. TEM images of aggregated structures illustrating thickening effects after addition of (a) 5 μg and (b) 15 μg of $PFDMS_{28}$ homopolymer added as 1 mg/mL solution in THF, (c) high-magnification TEM image of the area inside the red box shown in a, (d) high-magnification TEM image of the area inside the red box shown in b after thickening of the seed micelles has occurred. Tapping mode AFM height images of micelles (concentration 0.05 mg/mL) on freshly cleaved HOPG substrate after addition of (e) 5 μg and (f) 15 μg of $PFDMS_{28}$ homopolymer added as 1 mg/mL solution in THF (rms background: e = 0.40 nm; f = 0.26 nm), and (g) height profiles of end-coupled micelles from e (black) and networks of thickened micelles from f (green). Horizontal scale bars correspond to 500 nm. Vertical scale bars correspond to e = 0−20 nm, and f = 0−34 nm.

and 50 μg of $PFDMS_{28}$ homopolymer, no further increase in $R_{H,app}$ was detected.

From TEM analysis after solvent evaporation (Figure 3), the formation of increasingly dense aggregates from the short, cylindrical seed micelles was observed upon addition of larger quantities of homopolymer. The size of the aggregates was again much larger than suggested by DLS and is again consistent with the assertion that, although some aggregation occurs in solution, the majority may occur upon solvent evaporation. When only 5 μg of $PFDMS_{28}$ homopolymer was added, mainly end-to-end coupled cylindrical seed micelles were detected. However, a large number of single cylindrical seed micelles were also observed on the grids (Figure 3a). Increasing the quantity of $PFDMS_{28}$ homopolymer added to 10 μg resulted in an increase in the number of connections between seed micelles and ultimately in the formation of larger networks (Figure 3b). A similar increase in connectivity was evident when even more (i.e., 30 μg and 50 μg) $PFDMS_{28}$ homopolymer was added (Figure S8 of the Supporting Information).

Results from the AFM analysis of the micelle networks on an HOPG substrate (Figure S9 of the Supporting Information) also supported the formation of aggregates in which the added homopolymer primarily formed connections between the short, cylindrical seed micelles to give coupled structures. As the amount of added $PFDMS_{28}$ increased, more extensive networks were detected (Figure S9c of the Supporting Information). For the smallest quantity of added homopolymer (5 μg), unconnected, residual seed micelles of length ca. 200 nm were detected in addition to aggregates (Figure S9a of the Supporting Information). To confirm that network formation occurred as a result of micelle attachment rather than by the coincidental aggregation or overlapping of short, cylindrical seed micelles, we studied a selected linear coupled micelle structure by AFM (Figure 4). Figure 4c shows a height profile of the structure that provides compelling evidence that the short, cylindrical seed micelles are connected to each other rather than coincidentally overlapping randomly on the HOPG substrate (white arrows in the AFM height image (Figure 4a) illustrate higher features resulting from overlapping cylinders). This image confirms that six short, cylindrical seed micelles are connected linearly yielding the skeleton of a micelle structure ca. 1200 nm long that consists of coupled seed micelle subunits (Figure 4b, c).

In addition to the end-to-end coupling which yields long linear micelles and micelle networks, we also observed thickening of the core of the short, cylindrical seed micelles by TEM and AFM as shown in Figure 5. For example, most of the micelles shown in Figure 5b (15 μg of $PFDMS_{28}$ homopolymer added) are significantly thicker than those in Figure 5a (5 μg of $PFDMS_{28}$ added). The average thickness measured from TEM images of the micelles in Figure 5a and Figure 5b are ca. 20 nm and ca. 30 nm, respectively (see enlargements in Figure 5c and 5d). From the height profiles of the micelles (Figure 5g), it was also apparent that the micelles were thickened further if more homopolymer was added to the solution. It is therefore clear that not all of the added homopolymer appears at the cylinder ends and that competitive addition to the PFS core interface with the corona of the cylindrical seed micelles is also

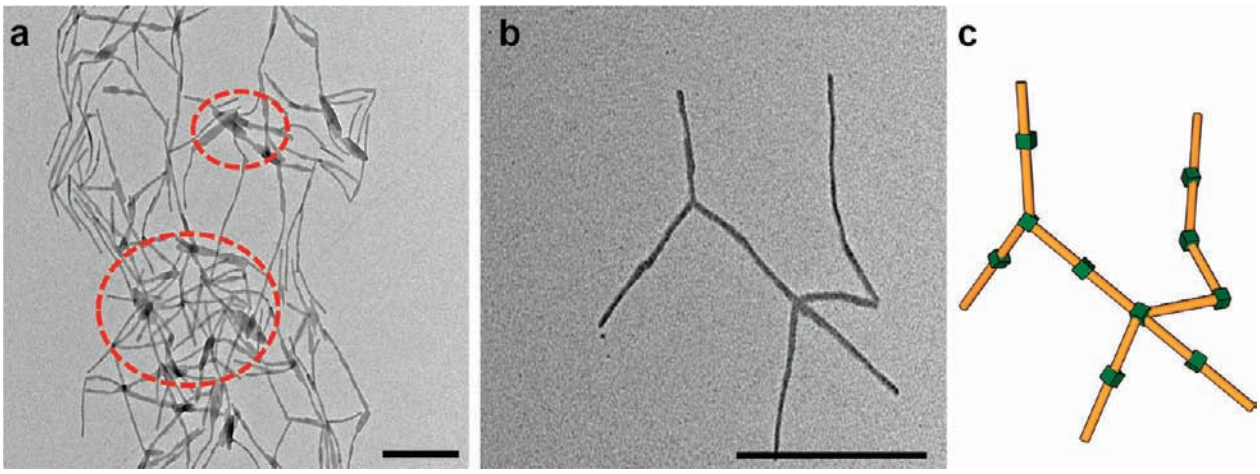

Figure 6. (a) TEM image of micelle networks after addition of 10 μg $PFDMS_{65}$ homopolymer added as 1 mg/mL solution in THF to short, cylindrical seed micelles of PI_{324}-*b*-$PFDMS_{54}$, (b) TEM image illustrating the homopolymer acting as glue in the formation of micelle networks, and (c) schematic representation of connected micelle seeds observed in Figure 6b. Scale bars correspond to 500 nm.

observed. Moreover, in cases where larger amounts of homopolymer were added, some remained in solution and formed a film on the substrate employed as observed by AFM (see Figure S10 of the Supporting Information).

2.2. Effect of the Molecular Weight of the Added PFDMS Homopolymer on the Aggregation of Short, Cylindrical Seed Micelles with a PFDMS Core. Next, we studied the effect of varying the molecular weight of the added PFDMS homopolymer on the aggregation process. TEM studies (Figure 6a) revealed that when 10 μg of $PFDMS_{65}$ (M_n = 15 700 g/mol; added as a 1 mg/mL solution in THF) was added, the micelles behaved in a similar fashion to those discussed previously for $PFDMS_{28}$. However, the higher molecular weight homopolymer showed an enhanced tendency to deposit and add at the end of the short, cylindrical seed micelles (red circles in Figure 6a). Figure 6b shows an example of added $PFDMS_{65}$ homopolymer apparently acting as a glue to connect several short, cylindrical seed micelles at their ends. Such interactions are likely to underlie the network formation observed in Figure 6a.

Very different behavior was observed when an even higher molecular weight homopolymer, $PFDMS_{141}$ (M_n = 34 200 g/mol), was added. This material immediately precipitated when it was added as a dilute THF solution to the *n*-hexane solution of cylindrical seed micelles precluding aggregation. The lack of end-to-end coupling or network formation was confirmed by DLS and TEM studies which revealed unchanged short seed micelles after addition of $PFDMS_{141}$ homopolymer (see Figure S11 of the Supporting Information). This is presumably due to the lower solubility of the high molecular weight $PFDMS_{141}$ homopolymer in *n*-hexane. These experiments suggest that PFDMS homopolymer can add to and couple the short, cylindrical seed micelles only below a certain molecular weight threshold which evidently corresponds to a value between those for $PFDMS_{65}$ and $PFDMS_{141}$. The studies also suggest that the addition and coupling by a more soluble, lower molecular weight homopolymer such as $PFDMS_{28}$ is most efficient with no evidence for extensive deposition detected at the seed termini.

2.3. Influence of Different Corona-Forming Blocks in the Short Cylindrical Seed Micelles on the Aggregation Induced by Added $PFDMS_{28}$ Homopolymer. To explore the effect of different corona-forming blocks on the aggregation behavior of the cylindrical seed micelles with added $PFDMS_{28}$ homopolymer, similar experiments were performed using short, cylindrical $PFDMS_{37}$-*b*-$PDMS_{258}$ block copolymer seed micelles and M(PFS_{37}-*b*-$PDMS_{258}$)-*b*-M(PI_{324}-*b*-PFS_{54})-*b*-M(PFS_{37}-*b*-$PDMS_{258}$) triblock comicelles (see Figure 7a) in place of the PI_{324}-*b*-$PFDMS_{54}$ seeds. The nomenclature used to describe the triblock comicelles is based on the abbreviation M for each micelle segment of the comicelle, which is in-turn comprised of the unique PFS based diblock copolymers identified in brackets.

Short, cylindrical $PFDMS_{37}$-*b*-$PDMS_{258}$ seed micelles (see Figure S12a of the Supporting Information) were prepared using previously published self-assembly protocols[12c,22] and possessed an average length of L_n = 200 nm (L_w/L_n = 1.03, σ/L_n = 0.15). We then studied the result from the addition of 10 μg of $PFDMS_{28}$ homopolymer (as 1 mg/mL solution in THF) to the cylindrical seed micelles of PFS_{37}-*b*-$PDMS_{258}$ in *n*-hexane. The results from TEM analysis showed that using seeds with different corona-forming blocks yielded similar micelle networks and core-thickening behavior to those discussed in the previous section (see Figure S12b of the Supporting Information).

The preparation of the M(PFS_{37}-*b*-$PDMS_{258}$)-*b*-M(PI_{324}-*b*-PFS_{54})-*b*-M(PFS_{37}-*b*-$PDMS_{258}$) triblock comicelles to be used as cylindrical seeds was achieved by the addition of 0.2 mg of $PFDMS_{37}$-*b*-$PDMS_{258}$ (10 mg/mL in THF) to 100 μg of sonicated PI_{324}-*b*-$PFDMS_{54}$ cylindrical micelle seeds (1 mg/mL in *n*-hexane, L_n = 200 nm, see Figure 1b for the seed micelles and Figure 7b for the triblock comicelles). The solution was diluted with 1 mL of *n*-hexane and subsequently was aged for 1 day. The resulting triblock comicelles were studied by TEM (Figure 7b), and this revealed cylindrical comicelles with a length L_n = 300 nm (L_w/L_n = 1.04, σ/L_n = 0.20). To study the effect of homopolymer addition, 20 μg of $PFDMS_{28}$ (as 1 mg/mL solution in THF) was added to M(PFS_{37}-*b*-$PDMS_{258}$)-*b*-M(PI_{324}-*b*-PFS_{54})-*b*-M(PFS_{37}-*b*-$PDMS_{258}$) triblock comicelles in *n*-hexane. The resulting TEM image illustrates that the micelle networks formed were also similar to those formed when $PFDMS_{28}$ was added to other PFS block copolymer seed micelles (Figure 7c).

2.4. Effect of the Addition of the Amorphous Homopolymer $PFEMS_{25}$ and the Crystalline Polyferrocenylgermane Homopolymer $PFDMG_{30}$ on the Aggregation Behavior for Short Cylindrical Seed Micelles of PI_{324}-*b*-$PFDMS_{54}$. In the previously described

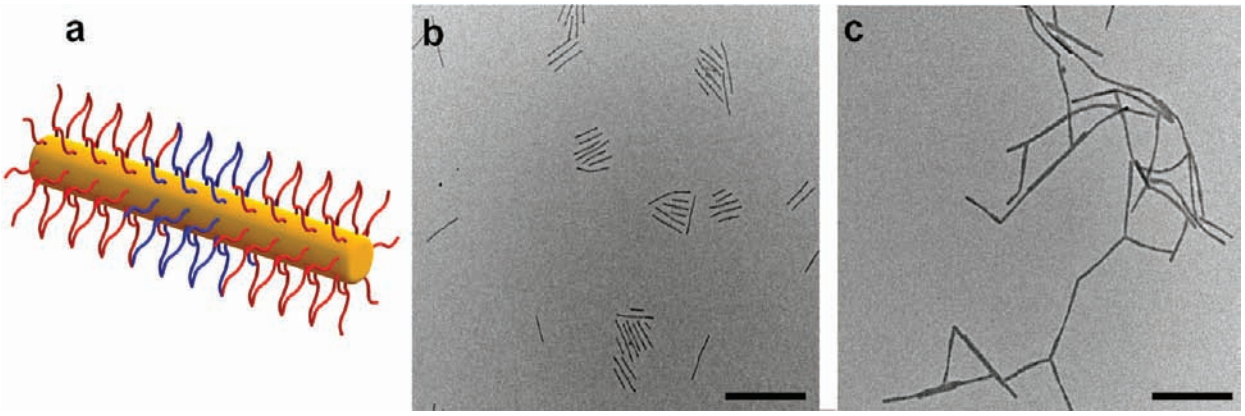

Figure 7. (a) Schematic representation M(PFS_{37}-*b*-$PDMS_{258}$)-*b*-M(PI_{324}-*b*-PFS_{54})-*b*-M(PFS_{37}-*b*-$PDMS_{258}$) triblock comicelles consisting of an amber PFS core, a blue PI corona, and a red PDMS corona, (b) TEM images of M(PFS_{37}-*b*-$PDMS_{258}$)-*b*-M(PI_{324}-*b*-PFS_{54})-*b*-M(PFS_{37}-*b*-$PDMS_{258}$) triblock comicelles used as seeds, and (c) micelle networks observed after addition of 20 μg of 1 mg/mL solution of $PFDMS_{28}$ homopolymer in THF to the triblock comicelles. Scale bars correspond to 500 nm.

experiments, semicrystalline PFDMS homopolymers were added to the crystalline core of short, cylindrical block copolymer seed micelles. To investigate if the crystallinity of the added homopolymer was essential for the observed aggregation behavior, we performed experiments in which the added homopolymer was not crystalline (i.e., amorphous) because of the unsymmetrical substitution pattern at the silicon bridge.[16f] For example, we added 30 μg of amorphous $PFEMS_{25}$ homopolymer (as 1 mg/mL solution in THF) to the short cylindrical PI_{324}-*b*-$PFDMS_{54}$ seed micelles and monitored the aggregation behavior using DLS and TEM. The $R_{H,app}$ value obtained from DLS experiments (see Figure S13 of the Supporting Information) indicated that, after addition of homopolymer, the micelles were similar in size to the original seed micelles, and subsequent TEM analysis after solvent evaporation also showed that the seed micelles remained unchanged. These results are consistent with the assertion that crystallinity is essential for the growth of homopolymer from the ends of the seed micelles.

As with the case of PFDMS, the germanium analog PFDMG (Scheme 2) has been shown to be semicrystalline.[26b] We performed experiments to explore potential epitaxial growth by adding 100 μg of $PFDMG_{30}$ homopolymer (as a 1 mg/mL solution in THF) to a solution of 200 nm cylindrical PI_{324}-*b*-$PFDMS_{54}$ seed micelles in *n*-hexane. The TEM results were not significantly different compared to those obtained when $PFDMS_{28}$ homopolymer was added except that fewer micelle networks formed even when the quantity of homopolymer added was increased to a maximum of 100 μg (Figure S14 of the Supporting Information). The micelle networks after addition of $PFDMG_{30}$ also showed that in many cases significant core thickening had occurred (average width ca. 40 nm) compared to the original seed micelles (average width ca. 20 nm). On this basis, the lattice parameters associated with PFDMG appear to be related closely enough for the heteroepitaxial growth of the homopolymer to occur at the crystalline micelle termini as has been previously observed[12b] on addition of PFDMG block copolymers with long corona-forming blocks to cylindrical PFS block copolymer seed micelles. In some cases, growth was also observed at the core−corona interface in these systems.

2.5. Effect of the Addition of PI-*b*-PFDMS Block Copolymer with Various Block Ratios to Short Cylindrical PI_{324}-*b*-PFS_{54} Seed Micelles. The studies described in the earlier sections involved the addition of PFDMS homopolymer to short cylindrical PI_{324}-*b*-$PFDMS_{54}$ seed micelles. These experiments led to promising end-to-end coupling but also to an associated amount of uncontrolled aggregation and network formation. Next, in an attempt to promote end-to-end coupling, we explored the addition of various PI-*b*-PFDMS block copolymers in place of PFDMS homopolymer to the seed micelles with the expectation that the presence of the solubilizing PI block might lead to more controlled deposition and assembly. Specifically, we examined the addition of PI-*b*-PFDMS block copolymers with various block ratios (6:1, 3.8:1, 2:1, and 1:1) to the PI_{324}-*b*-$PFDMS_{54}$ seed micelles.

A stirred hexane solution (1 mL) containing 80 μg of the cylindrical seed micelles was separately treated with 100 μg and 300 μg of PI_{324}-*b*-$PFDMS_{54}$, PI_{296}-*b*-$PFDMS_{77}$, PI_{200}-*b*-$PFDMS_{100}$, and PI_{76}-*b*-$PFDMS_{76}$ block copolymers in THF (10 mg/mL), and the samples were aged for 1 day before they were analyzed using TEM after solvent evaporation. TEM analysis (Figure 8a, b) showed that the addition of block copolymer with a long corona-forming block (PI_{324}-*b*-$PFDMS_{54}$; 6:1) to PI_{324}-*b*-$PFDMS_{54}$ seed micelles resulted in elongation of the original cylindrical seeds with the final length dependent on the quantity of PI_{324}-*b*-$PFDMS_{54}$ unimers added as demonstrated in previous publications.[12b,c] Similar results were obtained when PI_{296}-*b*-$PFDMS_{77}$ (3.8:1) was added confirming that cylinder elongation was also favored even at this lower corona to core block ratio (Figure 8c, d). AFM analysis (see Figure S15 of the Supporting Information) showed a significant difference in width (ca. 40 nm) between the middle region of the elongated cylinder, which corresponds to original seed micelle (Figure S15a and b of the Supporting Information), and the thicker outer regions that represent the new growth arising from the added block copolymer (Figure S15c and d of the Supporting Information). The results confirmed that even at a relatively low corona to core ratio of 3.8:1 in the added copolymer elongation at the end of the seed micelles was observed.

In contrast, the experiments involving the addition of PI_{200}-*b*-$PFDMS_{100}$ (block ratio 2:1) led to strikingly different behavior. This predominantly involved end-to-end coupling of the cylindrical seed micelles (Figure 8e, f) to generate linear aggregates, where core-thickening effects for the seeds appeared to be insignificant. Furthermore, unlike the experiments where added PFDMS homopolymer grew epitaxially from the ends of the seed micelles, a clear directional preference was detected.

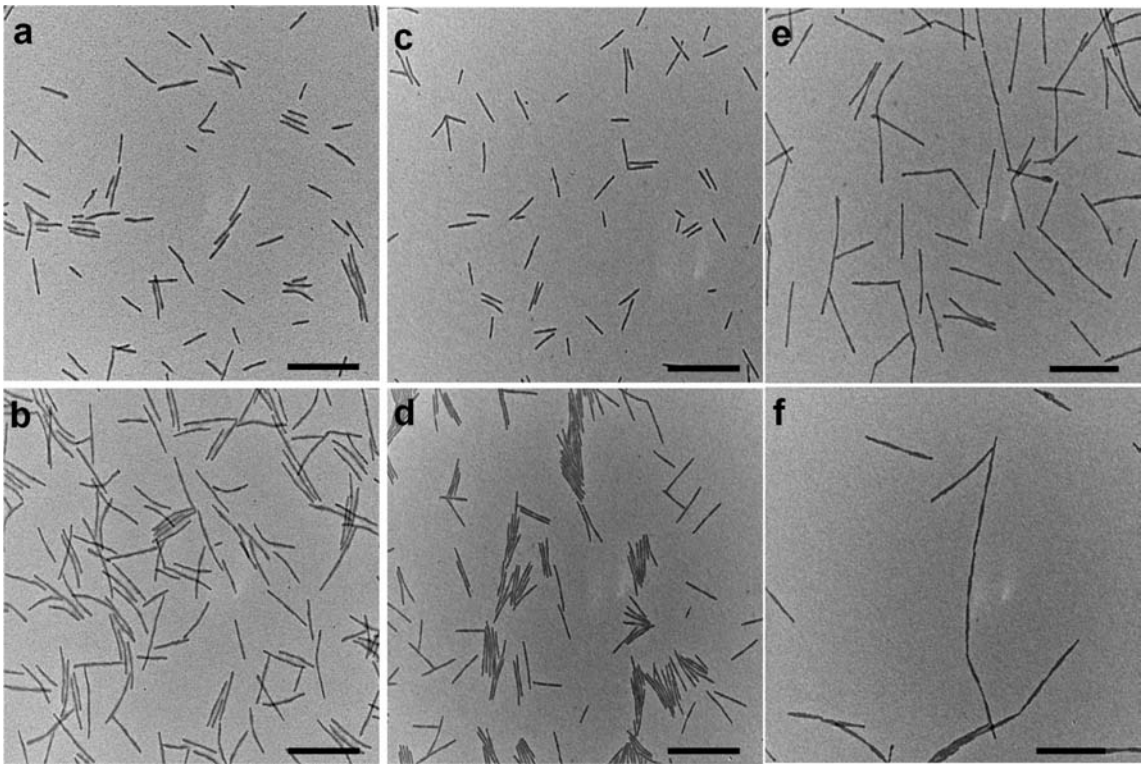

Figure 8. TEM images illustrating micelle growth after addition of (a) 100 μg (L_n = 290 nm, L_w/L_n = 1.15, σ/L_n = 0.45) and (b) 300 μg (L_n = 420 nm, L_w/L_n = 1.08, σ/L_n = 0.30) of PI_{324}-*b*-$PFDMS_{54}$ (block ratio 6:1), (c) 100 μg (L_n = 310 nm, L_w/L_n = 1.17, σ/L_n = 0.48) and (d) 300 μg (L_n = 390 nm, L_w/L_n = 1.10, σ/L_n = 0.43) of PI_{296}-*b*-$PFDMS_{77}$ (block ratio 3.8:1), (e) 100 μg and (f) 300 μg of PI_{200}-*b*-$PFDMS_{100}$ (block ratio 2:1) to 80 μg (1 mg/mL in *n*-hexane) of PI_{324}-*b*-$PFDMS_{54}$ short, cylindrical seed micelles. The block copolymers were added as 10 mg/mL solutions in THF. Scale bars correspond to 500 nm.

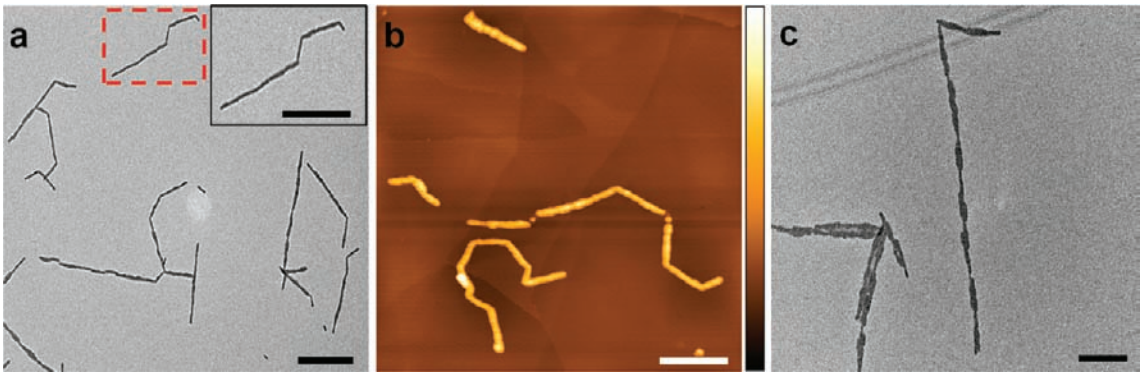

Figure 9. (a) TEM images (inset corresponds to a higher magnification image of the area inside the red box), (b) tapping mode AFM height image of micelle networks formed after addition of 100 μg of PI_{76}-*b*-$PFDMS_{76}$ added as a 10 mg/mL solution in THF, and (c) TEM image after addition of 300 μg of PI_{76}-*b*-$PFDMS_{76}$ added as a 10 mg/mL solution in THF to 80 μg of short cylindrical seed micelles of PI_{324}-*b*-$PFDMS_{54}$ in *n*-hexane (1 mg/mL). See Figure S16 of the Supporting Information for a higher magnification of the TEM image of the aggregates shown in c. The AFM sample was prepared by drop casting of micelle solution (concentration 0.03 mg/mL) onto freshly cleaved HOPG (rms background 0.76 nm). Horizontal scale bars correspond to 500 nm. Vertical scale bar in b corresponds to 0−16 nm.

TEM and AFM (Figure 9) analysis of the coupled structures formed upon the analogous addition of the symmetric block copolymer PI_{76}-*b*-$PFDMS_{76}$ (1:1) to the short cylindrical PI_{324}-*b*-$PFDMS_{54}$ seed micelles also revealed the presence of linear micelle aggregates (Figure 9a). Even when large amounts of unimers were added, linear aggregates were still predominantly formed (Figure 9c) although significant thickening was detected for the connecting segments that represent new growth in this case (see Figures S16 and 17 of the Supporting Information).[29] This thickening behavior was not detected upon addition of the 2:1 PI-*b*-PFDMS block copolymer under similar conditions (Figure 8f).

Overall, the addition of PI-*b*-PFDMS block copolymers with a block ratio of 2:1 or, less impressively, 1:1, led to much more controlled aggregation than that observed with PFDMS homopolymer with less branching and network formation observed

and very few remaining uncoupled seeds. It is possible that the predominantly linear end-to-end coupling detected in a direction along the long axis of the seed micelle is a result of a tendency to limit the steric interactions between the PI corona on the seed and that derived from the added block copolymer in the region of new growth.

SUMMARY

The addition of the crystalline polyferrocenylsilane homopolymer (PFDMS) to short, cylindrical block copolymer seed micelles with a PFDMS core led to aggregation as a result of end-to-end coupling and also micelle network formation. Deposition and crystallization of homopolymer at the ends of the cylindrical seed micelles led to end-to-end coupling of two or more micelles to give linear, linked, or branched structures. Furthermore, deposition along the seed micelles at the core–corona interface led to significant micelle thickening as detected by TEM and AFM. Network formation appeared to partly result from subsequent micelle attachment along the length of the seed micelles. In contrast, no end-to-end coupling or network formation was detected when the amorphous homopolymer PFEMS was added in place of PFDMS, which is consistent with an epitaxial growth mechanism. Further support for this assertion was provided by the observation of end-to-end coupling and network formation when crystalline polyferrocenylgermane homopolymer (PFDMG) was added to the cylindrical seeds.

Strikingly different behavior was detected upon the addition of PI-*b*-PFDMS block copolymers (block ratios 6:1, 3.8:1, 2:1, and 1:1) to the short cylindrical seed micelles. This ranged from typical micelle elongation detected previously[12b,c] at high corona to core-forming block ratios (PI-*b*-PFDMS; 6:1 and 3.8:1) to predominantly end-to-end coupling at lower ratios (PI-*b*-PFDMS; 2:1 and 1:1). For the latter cases, especially for the 2:1 block copolymer, this led to the predominant formation of long, well-defined linear end-to-end coupled structures (e.g., Figures 8e, f and 9a and b) and represented the most controlled aggregation processes found in this study. The preferential and more controlled deposition and crystallization of these materials at the seed micelle termini and the resulting formation of predominantly linear aggregates is likely a result of the presence of the solubilizing and sterically significant PI coblock. The phenomena described may also be applicable to other cylindrical micelle systems with a crystalline core,[23,30] including those based on π-conjugated materials.[30] This may allow the formation of well-defined, functional linear assemblies by controlled end-to-end coupling using a method that draws interesting parallels with processes that have been recently developed to assemble inorganic nanoparticles.[31]

ASSOCIATED CONTENT

Supporting Information. Full experimental details and characterization including additional DLS, AFM, and TEM data. This material is available free of charge via the Internet at http://pubs.acs.org.

AUTHOR INFORMATION

Corresponding Authors

mwinnik@chem.utoronto.ca; ian.manners@bristol.ac.uk

ACKNOWLEDGMENTS

S.F.M.Y. is grateful to the Ministry of Higher Education of Malaysia and Universiti Kebangsaan Malaysia for the provision of a Ph.D scholarship, and J.B.G. thanks the NSERC of Canada and the European Union Marie Curie Program for postdoctoral fellowships. I.M. thanks the European Union for a Marie Curie Chair, the European Research Council for an Advanced Investigator Grant, and the Royal Society for a Wolfson Research Merit Award. M.A.W. also thanks the NSERC of Canada for financial support. We also thank Dr. Felix H. Schacher for helpful discussions and suggestions, Dr. Paul A. Rupar for preparing micelle graphics, and Dr. Torben Gädt for preparing PI_{76}-*b*-$PFDMS_{76}$.

REFERENCES

(1) (a) Jang, Y. H.; Kochuveedu, S. T.; Cha, M.-A.; Jang, Y. J.; Lee, J. Y.; Lee, J.; Lee, J.; Kim, J.; Ryu, D. Y.; Kim, D. H. *J. Colloid Interface Sci.* **2010**, *345*, 125–130. (b) Tang, C.; Hur, S.-M.; Stahl, B. C.; Sivanandan, K.; Dimitriou, M.; Pressly, E.; Fredrickson, G. H.; Kramer, E. J.; Hawker, C. J. *Macromolecules* **2010**, *43*, 2880–2889. (c) Kong, W.; Li, B.; Jin, Q.; Ding, D.; Shi, A.-C. *Langmuir* **2010**, *26*, 4226–4232. (d) Sriprom, W.; Neto, C.; Perrier, S. *Soft Matter* **2010**, *6*, 909–914. (e) Qian, J.; Zhang, M.; Manners, I.; Winnik, M. A. *Trends Biotechnol.* **2010**, *28*, 84–92. (f) Hayward, R. C.; Pochan, D. J. *Macromolecules* **2010**, *43*, 3577–3584.

(2) (a) Alexandridis, P.; Lindman, B. *Amphiphilic Block Copolymers: Self-Assembly and Applications*; Elsevier: New York, 2000. (b) Krausch, G.; Magerle, R. *Adv. Mater.* **2002**, *14*, 1579–1583. (c) Park, C.; Yoon, J.; Thomas, E. L. *Polymer* **2003**, *44*, 6725–6760. (d) Cheng, J. Y.; Mayes, A. M.; Ross, C. A. *Nat. Mater.* **2004**, *3*, 823–828. (e) Runge, M. B.; Lipscomb, C. E.; Ditzler, L. R.; Mahanthappa, M. K.; Tivanski, A. V.; Bowden, N. B. *Macromolecules* **2008**, *41*, 7687–7694. (f) Eloi, J.-C.; Rider, D. A.; Wang, J.-Y.; Russell, T. P.; Manners, I. *Macromolecules* **2008**, *41*, 9474–9479. (g) Chuang, V. P.; Gwyther, J.; Mickiewicz, R. A.; Manners, I.; Ross, C. A. *Nano Lett.* **2009**, *9*, 4364–4369. (h) Gwyther, J.; Manners, I. *Polymer* **2009**, *50*, 5384–5389. (i) Bang, J.; Jeong, U.; Ryu, D. Y.; Russell, T. P.; Hawker, C. J. *Adv. Mater.* **2009**, *21*, 4769–4792.

(3) (a) Hashimoto, K.; Sugata, T.; Mashita, A.; Okada, M. *J. Appl. Polym. Sci.* **1994**, *53*, 915–922. (b) Ludwigs, S.; Böker, A.; Voronov, A.; Rehse, N.; Magerle, R.; Krausch, G. *Nat. Mater.* **2003**, *2*, 744–747. (c) Fu, G. D.; Kang, E. T.; Neoh, K. G. *Langmuir* **2005**, *21*, 3619–3624.

(4) (a) Lyuksyutov, S. F.; Vaia, R. A.; Paramonov, P. B.; Juhl, S.; Waterhouse, L.; Ralich, R. M.; Sigalov, G.; Sancaktar, E. *Nat. Mater.* **2003**, *2*, 468–472. (b) Park, M.; Harrison, C.; Chaikin, P. M.; Register, R. A.; Adamson, D. H. *Science* **1997**, *276*, 1401–1404. (c) Jung, Y. S.; Chang, J. B.; Verploegen, E.; Berggren, K. K.; Ross, C. A. *Nano Lett.* **2010**, *10*, 1000–1005.

(5) (a) Urbas, A. M.; Maldovan, M.; DeRege, P.; Thomas, E. L. *Adv. Mater.* **2002**, *14*, 1850–1853. (b) Lu, Y.; Xia, H.; Zhang, G.; Wu, C. *J. Mater. Chem.* **2009**, *19*, 5952–5955. (c) Deng, T.; Chen, C.; Honeker, C.; Thomas, E. L. *Polymer* **2003**, *44*, 6549–6553.

(6) (a) Zhang, L.; Eisenberg, A. *Science* **1995**, *268*, 1728–1731. (b) Peng, H.; Chen, D.; Jiang, M. *Macromolecules* **2005**, *38*, 3550–3553. (c) Discher, D. E.; Eisenberg, A. *Science* **2002**, *297*, 967–973. (d) Jain, S.; Bates, F. S. *Science* **2003**, *300*, 460–464. (e) Liu, G.; Ding, J.; Qiao, L.; Guo, A.; Dymov, B. P.; Gleeson, J. T.; Hashimoto, T.; Saijo, K. *Chem.—Eur. J.* **1999**, *5*, 2740–2749. (f) Fu, J.; Luan, B.; Yu, X.; Cong, Y.; Li, J.; Pan, C.; Han, Y.; Yang, Y.; Li, B. *Macromolecules* **2004**, *37*, 976–986. (g) Chen, Z.; Cui, H.; Hales, K.; Li, Z.; Qi, K.; Pochan, D. J.; Wooley, K. L. *J. Am. Chem. Soc.* **2005**, *127*, 8592–8593. (h) Bang, J.; Jain, S.; Li, Z.; Lodge, T. P.; Pedersen, J. S.; Kesselman, E.; Talmon, Y. *Macromolecules* **2006**, *39*, 1199–1208. (i) Walther, A.; Drechsler, M.; Rosenfeldt, S.; Harnau, L.; Ballauff, M.; Abetz, V.; Müller, A. H. E. *J. Am. Chem. Soc.* **2009**, *131*, 4720–4728. (j) Zhu, J.; Hayward, R. C. *J. Am. Chem. Soc.* **2008**, *130*, 7496–7502.

(7) (a) Förster, S.; Antonietti, M. *Adv. Mater.* **1998**, *10*, 195–217. (b) Bouilhac, C.; Cloutet, E.; Taton, D.; Deffieux, A.; Borsali, R.; Cramail, H. *J. Polym. Sci., Part A: Polym. Chem.* **2009**, *47*, 197–209. (c) Braun, C. H.; Richter, T. V.; Schacher, F.; Müller, A. H. E.; Crossland, E. J. W.; Ludwigs, S. *Macromol. Rapid Commun.* **2010**, *31*, 729–734. (d) Yan, X.; Liu, G.; Haeussler, M.; Tang, B. Z. *Chem. Mater.* **2005**, *17*, 6053–6059.

(8) (a) Geng, Y.; Dalhaimer, P.; Cai, S.; Tsai, R.; Tewari, M.; Minko, T.; Discher, D. E. *Nat. Nanotechnol.* **2007**, *2*, 249–255. (b) Kim, Y.; Dalhaimer, P.; Christian, D. A.; Discher, D. E. *Nanotechnology* **2005**, *16*, S484–S491. (c) Chiappetta, D. A.; Sosnik, A. *Eur. J. Pharm. Biopharm.* **2007**, *66*, 303–317.

(9) Lu, J.; Yi, S. S.; Kopley, T.; Qian, C.; Liu, J.; Gulari, E. *J. Phys. Chem. B* **2006**, *110*, 6655–6660.

(10) (a) Bellas, V.; Rehahn, M. *Angew. Chem., Int. Ed.* **2007**, *46*, 5082–5104. (b) Herbert, D. E.; Mayer, U. F. J.; Manners, I. *Angew. Chem., Int. Ed.* **2007**, *46*, 5060–5081. (c) Manners, I. *Can. J. Chem.* **1998**, *76*, 371–381. (d) Whittell, G. R.; Hager, M. D.; Schubert, U. S.; Manners, I. *Nat. Mater.* **2011**, *10*, 176–188.

(11) (a) Rider, D. A.; Cavicchi, K. A.; Vanderark, L.; Russell, T. P.; Manners, I. *Macromolecules* **2007**, *40*, 3790–3796. (b) Korczagin, I.; Lammertink, R. G. H.; Hempenius, M. A.; Golze, S.; Vancso, G. J. *Adv. Polym. Sci.* **2006**, *200*, 91–117. (c) Rider, D. A.; Liu, K.; Eloi, J.-C.; Vanderark, L.; Yang, L.; Wang, J.-Y.; Grozea, D.; Lu, Z.-H.; Russell, T. P.; Manners, I. *ACS Nano* **2008**, *2*, 263–270. (d) Li, J. K.; Zou, S.; Rider, D. A.; Manners, I.; Walker, G. C. *Adv. Mater.* **2008**, *20*, 1989–1993. (e) Ramanathan, M.; Nettleton, E.; Darling, S. B. *Thin Solid Films* **2009**, *517*, 4474–4478. (f) Xu, J.; Bellas, V.; Jungnickel, B.; Stühn, B.; Rehahn, M. *Macromol. Chem. Phys.* **2010**, *211*, 1261–1271.

(12) (a) Wang, X.; Guerin, G.; Wang, H.; Wang, Y.; Manners, I.; Winnik, M. A. *Science* **2007**, *317*, 644–647. (b) Gädt, T.; Ieong, N. S.; Cambridge, G.; Winnik, M. A.; Manners, I. *Nat. Mater.* **2009**, *8*, 144–150. (c) Gilroy, J. B.; Gädt, T.; Whittell, G. R.; Chabanne, L.; Mitchels, J. M.; Richardson, R. M.; Winnik, M. A.; Manners, I. *Nat. Chem.* **2010**, *2*, 566–570.

(13) (a) Cheng, J. Y.; Ross, C. A.; Chan, V. Z.-H.; Thomas, E. L.; Lammertink, R. G. H.; Vancso, G. J. *Adv. Mater.* **2001**, *13*, 1174–1178. (b) Lu, J.; Chamberlin, D.; Rider, D. A.; Liu, M.; Manners, I.; Russell, T. P. *Nanotechnology* **2006**, *17*, 5792–5797. (c) Lammertink, R. G. H.; Hempenius, M. A.; van den Enk, J. E.; Chan, V. Z.-H.; Thomas, E. L.; Vancso, G. J. *Adv. Mater.* **2000**, *12*, 98–103.

(14) (a) Wang, X.-S.; Wang, H.; Coombs, N.; Winnik, M. A.; Manners, I. *J. Am. Chem. Soc.* **2005**, *127*, 8924–8925. (b) Rider, D. A.; Winnik, M. A.; Manners, I. *Chem. Commun.* **2007**, 4483–4485.

(15) (a) Lu, J. Q.; Kopley, T. E.; Moll, N.; Roitman, D.; Chamberlin, D.; Fu, Q.; Liu, J.; Russell, T. P.; Rider, D. A.; Manners, I.; Winnik, M. A. *Chem. Mater.* **2005**, *17*, 2227–2231. (b) Hinderling, C.; Keles, Y.; Stöckli, T.; Knapp, H. F.; De los Arcos, T.; Oelhafen, P.; Korczagin, I.; Hempenius, M. A.; Vancso, G. J.; Pugin, R.; Heinzelmann, H. *Adv. Mater.* **2004**, *16*, 876–879. (c) Lastella, S.; Jung, Y. J.; Yang, H.; Vajtai, R.; Ajayan, P. M.; Ryu, C. Y.; Rider, D. A.; Manners, I. *J. Mater. Chem.* **2004**, *14*, 1791–1794.

(16) (a) Rider, D. A.; Chen, J. I. L.; Eloi, J.-C.; Arsenault, A. C.; Russell, T. P.; Ozin, G. A.; Manners, I. *Macromolecules* **2008**, *41*, 2250–2259. (b) Roerdink, M.; Hempenius, M. A.; Vancso, G. J. *Chem. Mater.* **2005**, *17*, 1275–1278. (c) Wang, H.; Winnik, M. A.; Manners, I. *Macromolecules* **2007**, *40*, 3784–3789. (d) Wang, Y.; Coombs, N.; Manners, I.; Winnik, M. A. *Macromol. Chem. Phys.* **2008**, *209*, 1432–1436. (e) Lammertink, R. G. H.; Hempenius, M. A.; Thomas, E. L.; Vancso, G. J. *J. Polym. Sci., Part B: Polym. Phys.* **1999**, *37*, 1009–1021. (f) Rider, D. A.; Cavicchi, K. A.; Power-Billard, K. N.; Russell, T. P.; Manners, I. *Macromolecules* **2005**, *38*, 6931–6938. (g) Massey, J.; Power, K. N.; Manners, I.; Winnik, M. A. *J. Am. Chem. Soc.* **1998**, *120*, 9533–9540.

(17) Ramanathan, M.; Darling, S. B. *Soft Matter* **2009**, *5*, 4665–4671.

(18) Shen, L.; Wang, H.; Guerin, G.; Wu, C.; Manners, I.; Winnik, M. A. *Macromolecules* **2008**, *41*, 4380–4389.

(19) (a) Wang, X.; Liu, K.; Arsenault, A. C.; Rider, D. A.; Ozin, G. A.; Winnik, M. A.; Manners, I. *J. Am. Chem. Soc.* **2007**, *129*, 5630–5639. (b) Korczagin, I.; Hempenius, M. A.; Fokkink, R. G.; Cohen Stuart, M. A.; Al-Hussein, M.; Bomans, P. H. H.; Frederik, P. M.; Vancso, G. J. *Macromolecules* **2006**, *39*, 2306–2315. (c) Wurm, F.; Hilf, S.; Frey, H. *Chem.—Eur. J.* **2009**, *15*, 9068–9077.

(20) Cao, L.; Manners, I.; Winnik, M. A. *Macromolecules* **2002**, *35*, 8258–8260.

(21) (a) Papkov, V. S.; Gerasimov, M. V.; Dubovik, I. I.; Sharma, S.; Dementiev, V. V.; Pannell, K. H. *Macromolecules* **2000**, *33*, 7107–7115. (b) Lammertink, R. G. H.; Hempenius, M. A.; Manners, I.; Vancso, G. J. *Macromolecules* **1998**, *31*, 795–800. (c) Xu, J.; Ma, Y.; Hu, W.; Rehahn, M.; Reiter, G. *Nat. Mater.* **2009**, *8*, 348–353.

(22) Massey, J. A.; Temple, K.; Cao, L.; Rharbi, Y.; Raez, J.; Winnik, M. A.; Manners, I. *J. Am. Chem. Soc.* **2000**, *122*, 11577–11584.

(23) (a) Portinha, D.; Boué, F.; Bouteiller, L.; Carrot, G.; Chassenieux, C.; Pensec, S.; Reiter, G. *Macromolecules* **2007**, *40*, 4037–4042. (b) Schmalz, H.; Schmelz, J.; Drechsler, M.; Yuan, J.; Walther, A.; Schweimer, K.; Mihut, A. M. *Macromolecules* **2008**, *41*, 3235–3242. (c) Lazzari, M.; Scalarone, D.; Vazquez-Vazquez, C.; López-Quintela, M. A. *Macromol. Rapid Commun.* **2008**, *29*, 352–357. (d) Du, Z.-X.; Xu, J.-T.; Fan, Z.-Q. *Macromol. Rapid Commun.* **2008**, *29*, 467–471. (e) Mihut, A. M.; Drechsler, M.; Möller, M.; Ballauff, M. *Macromol. Rapid Commun.* **2010**, *31*, 449–453. (f) Zhang, J.; Wang, L.-Q.; Wang, H.; Tu, K. H. *Biomacromolecules* **2006**, *7*, 2492–2500. (g) Petzetakis, N.; Dove, A. P.; O'Reilly, R. K. *Chem. Sci.* **2011**, *2*, 955–960.

(24) (a) Gast, A. P.; Vinson, P. K.; Cogan-Farinas, K. A. *Macromolecules* **1993**, *26*, 1774–1776. (b) Lotz, B.; Kovacs, A. J.; Bassett, G. A.; Keller, A. *Colloid Polym. Sci.* **1966**, *209*, 115–128. (c) Richter, D.; Schneiders, D.; Monkenbusch, M.; Willner, L.; Fetters, L. J.; Huang, J. S.; Lin, M.; Mortensen, K.; Farago, B. *Macromolecules* **1997**, *30*, 1053–1068. (d) Ramzi, A.; Prager, M.; Richter, D.; Efstratiadis, V.; Hadjichristidis, N.; Young, R. N.; Allgaier, J. B. *Macromolecules* **1997**, *30*, 7171–7182. (e) Lin, E. K.; Gast, A. P. *Macromolecules* **1996**, *29*, 4432–4441.

(25) (a) Wang, H.; Patil, A. J.; Liu, K.; Petrov, S.; Mann, S.; Winnik, M. A.; Manners, I. *Adv. Mater.* **2009**, *21*, 1805–1808. (b) Wang, H.; Lin, W.; Fritz, K. P.; Scholes, G. D.; Winnik, M. A.; Manners, I. *J. Am. Chem. Soc.* **2007**, *129*, 12924–12925.

(26) (a) Ni, Y.; Rulkens, R.; Manners, I. *J. Am. Chem. Soc.* **1996**, *118*, 4102–4114. (b) Ieong, N. S.; Manners, I. *Macromol. Chem. Phys.* **2009**, *210*, 1080–1086. (c) Foucher, D. A.; Edwards, M.; Burrow, R. A.; Lough, A. J.; Manners, I. *Organometallics* **1994**, *13*, 4959–4966.

(27) The aggregation observed in solution is also apparently irreversible. When the micelle solution was diluted by a factor of up to 50 and then left for 12 h, the larger aggregates were still detected by DLS. See Figure S6 of the Supporting Information for details.

(28) As the DLS measurements afford hydrodynamic size based on a solid sphere model ($R_{H,app}$), the data would be expected to be only qualitative for cylinders and their aggregates. Nevertheless, the disparity between the size of the aggregates detected by DLS and TEM/AFM is so large that this approximation is not logical as the main explanation for the difference detected.

(29) We also studied the addition of PI_{76}-*b*-PFS_{76} (1:1) to longer seed micelles ($L_n \sim 500$ nm), and similar results were obtained. See Supporting Information, including Figure S18, for details.

(30) Patra, S. K.; Ahmed, R.; Whittell, G. R.; Lunn, D. J.; Dunphy, E. L.; Winnik, M. A.; Manners, I. *J. Am. Chem. Soc.* **2011**, *133*, 8842–8845.

(31) Liu, K.; Nie, Z.; Zhao, N.; Li, W.; Rubinstein, M.; Kumacheva, E. *Science* **2010**, *329*, 197–200.